Journal of Reinforced Plastics and Composites

Interfacial and mechanical properties of polypropylene/silica nano- and microcomposites

A Pustak, M Leskovac, M Denac, I Svab, J Pohleven, M Makarovic, V Musil and I Smit

Published by:

$SAGE

http://www.sagepublications.com

Additional services and information for *Journal of Reinforced Plastics and Composites* can be found at:

Email Alerts: http://jrp.sagepub.com/cgi/alerts

Subscriptions: http://jrp.sagepub.com/subscriptions

Reprints: http://www.sagepub.com/journalsReprints.nav

Permissions: http://www.sagepub.com/journalsPermissions.nav

>> OnlineFirst Version of Record - Jan 16, 2014

What is This?

Interfacial and mechanical properties of polypropylene/silica nano- and microcomposites

A Pustak[1], M Leskovac[2], M Denac[3], I Švab[4], J Pohleven[3], M Makarovič[5], V Musil[3] and I Šmit[1]

Abstract
Various silica grades differing in particle size (micro- versus nanosilica) and surface modification (untreated versus modified surface) have affected interfacial and mechanical properties of compression-molded polypropylene composites with 2, 4, 6, 8 vol% of added silica. Mechanical properties have been influenced primarily by combination of stiff fillers and tough polypropylene matrix and additionally by restructured matrix. Namely, silica particles with different surface properties have influenced nucleation and spherulite growth differently affecting thus tensile properties of the composites. All composites exhibited best tensile strength in silica content range 2–6 vol%.

Keywords
Mechanical properties, interfacial properties, polymer–matrix composites, polypropylene, silica

Introduction

Production and use of polymer–matrix composites has become fast-growing field of research due to a favorable cost/performance ratio.[1–4] As one of the most widely used plastomer, isotactic polypropylene (iPP) offered favorable combination of many factors in composite materials besides a good balance in physical and chemical properties. On the other hand, synthetic silica fillers offered some improvements in terms of processability and mechanical properties of polymer composites.[1–4] Although the structure–property relationships is a major target of materials scientists, these relationships in polymer composites are hardly universal and require a multiscale approach.[5] Due to mostly specific nature of these relationships in particular polymer composites, the investigations of these composites are often focused on specific goals taking into account all factors influencing the ultimate properties of polymer composites: characteristics of the fillers, filler loadings, and interaction between matrix and filler particle as well as between fillers particles within polymer matrix.[2–5]

Accordingly, the investigations of binary iPP/silica composites were mainly focused on two aims: preparation of new composite materials with improved

mechanical properties and crystallization study of the iPP/silica composites. Improving of mechanical properties in polymer composites has been focused mainly on reduction of silica particle agglomeration by surface treatment even by grafting of polymers onto filler particles improving thus silica particle dispersion, distribution, and polymer–filler interactions.[6–10] The considerations taking account all of these factors concerning amorphous polymer matrix may be quite satisfied. In the case of amorphous polymers, it could

[1]Division of Materials Chemistry, Ruđer Bošković Institute, Bijenička, Zagreb, Croatia
[2]Faculty of Chemical Engineering and Technology, University of Zagreb, Savska, Zagreb, Croatia
[3]University of Maribor, FEB Maribor, Institute of Technology, Razlagova, Maribor, Slovenia
[4]ISOKON, Production and Processing of Thermoplastics, Slovenske, Konjice, Slovenia
[5]ZAG, Slovenian National Building and Civil Engineering Institute, Dimičeva, Ljubljana, Slovenia

Corresponding author:
Anđela Pustak, Division of Materials Chemistry, Ruđer Bošković Institute, Bijenička 54, 10002 Zagreb, Croatia.
Email: apustak@irb.hr

Table 1. Filler characteristics.

Samples	Trade name of filler	Tapped density (g/l)	Surface modified	Specific surface area (m²/g)	Particle size, d_{50}
A-200	Aerosil 200; unmodified nanosilica	~50	None	200 [a]	12 nm
A-R7200	Aerosil R7200; modified nanosilica	~230	Methacrylsilane	150 [a]	12 nm
A-R8200	Aerosil R8200; modified nanosilica	140	Hexamethyl-disilazane	160 [a]	12 nm
S-120	Sipernat 120; unmodified microsilica	185	None	125 [b]	14.5 μm
S-D17	Sipernat D17; modified microsilica	150	2% chemically bounded carbon	100 [b]	10 μm

[a]BET (Brunauer, Emmett and Teller) method.
[b]measured by aerometer.

be possible even to predict tensile properties on the basis of adhesion between polymer matrix and filler.[11] However, in the case of semicrystalline polymer like iPP it should consider the structural and morphological changes of crystalline polymer matrix by incorporated additives.[2–5,12–15] Namely, filler particles with different characteristics (size, shape, and surface) may nucleate different crystal iPP phase (α, β, γ, smectic) as well as isotropic or oriented crystallite and spherulite growth and consequently, final morphology (spherulitic, grain, etc.) of the composites. Accordingly, modeling of optimal mechanical properties of polymer composites could be achieved by researching their structure–property relationships. The structural and morphological characteristics of nonisothermally crystallized compression molded iPP/silica within the contexts of structure–property relationships have been presented in previous paper.[15] It was established that silica surface properties exhibited stronger effects on the spherulitic morphology than size of silica particles, while phase structure of the iPP matrix is mainly unaffected. This paper is thorough study dealing with interfacial and mechanical properties and their relations with ultimate morphology in the context of structure–property relationships. The research was carried out with silica fillers differing in size (nano- versus micro-) and surface properties (hydrophilic versus hydrophobic, e.g. polar versus nonpolar). The effects of different silica fillers characteristics and content on polymer matrix and mechanical properties of composites will be discussed in this paper.

Experimental

Materials

The materials used in this study were iPP and five types of commercial silica fillers. The iPP used for sample preparation was Moplen HP501L, LyondellBasell Industries, Rotterdam, Netherlands (melt flow rate (230°C/2.16 kg) = 6 g/10 min, $\rho = 0.90$ g/cm³, $M_n = 120{,}000$ g/mol[1]). Silica fillers were two proprietary microsilicas (unmodified S-120 and surface modified S-D17) and three proprietary nanosilicas (unmodified A-200 and two surface modified silicas A-R7200 and A-R8200); all silica grades were kindly supplied by Evonic Industries (Degussa AG), Essen, Germany. Filler characteristics are listed in Table 1.

Samples preparation

Binary iPP/silica composites with volume content ratios 100/0, 98/2, 96/4, 94/6, and 92/8 were prepared in an oil-heated Brabender kneading chamber. The components were put in the chamber preheated up to 200°C with a rotor speed of 50 per min. The components were kneaded for 7 min. After homogenization, the melt was rapidly transferred to a preheated laboratory press and compression molded into 1- and 4-mm thick plates. The pressing temperature was 220°C, pressure 100 bar, and the pressing time 14 min for 1-mm thick plate and 11.5 min for 4-mm thick plate.

Testing methods

Steady state torque moment. The mixing torque value (τ_M) was determined from the diagram of kneading in the Brabender kneading chamber. The average τ_M value was calculated on the basis of five measurements carried out for each sample.

Tensile tests. Tensile properties (Young's modulus, yield stress, elongation at yield stress, tensile strength at break, elongation at break) were measured according to ISO 527 using Zwick 147670 Z100/SN5A apparatus at 23°C and a strain rate of 2 mm/min. For each sample, five measurements were taken and average values calculated within standard deviation of 5%.

Interaction parameter B could be calculated from the yield stress values. The extent of interfacial interactions in polypropylene/silica composites could be

evaluated by semiempirical equation (1) derived by Turcsányi et al.[16]

$$\sigma_{yc} = \sigma_{yp} \frac{1 - \phi_f}{1 + 2.5\phi_f} \exp(B\phi_f) \qquad (1)$$

where σ_{yc} and σ_{yp} are yield stress of the composite and polymer matrix, respectively, while ϕ_f is the volume fraction of filler, and B is a parameter which indicates the interfacial interactions in the composites. If $\ln[\sigma_{yc}(1 + 2.5\phi_f)/(\sigma_{yp}(1-\phi_f)]$ of fraction value is plotted against ϕ_f of silica dispersed phase, parameter B can be calculated as a line slope, with intercept in cross section of coordinate parameter axes. This assumes a tensile yield stress of matrix (σ_{yp}) to be constant.

Notched impact strength. Notched impact strength was measured by Zwick apparatus at 25°C according to Charpy test (DIN 53453). For each sample, 12 measurements were carried out and the average values were calculated within the standard deviation of 5%.

Contact angle measurement. Surface free energies, as well as the corresponding dispersive and polar component of materials, were determined by measuring the contact angles. The contact angles of the iPP and silica fillers were measured on a contact angle goniometer Data Physics OCA 20 Instrument at a temperature of 23°C. Sessile drops (2 μl) of test liquids: water (twice distilled $\lambda = 1.33\,\mu l/cm^1$), formamide (p.a. 99.5%, Fluka), and diiodomethane (p.a. 99%, Aldrich), at 23°C were used for the advancing contact angle measurements. The surface tensions of the test liquids[17] used for the contact angle measurements are presented in Table 2.

Surface free energies of the iPP and silica fillers (γ_{lv}) were calculated using the harmonic mean equation from the measured contact angles (θ) and the known values of the surface free energy used for the test liquids (Table 2) according to the Wu model[18] (equation (2))

$$\gamma_{lv}(1 + \cos(\theta)) = \frac{4\gamma_s^d \gamma_{lv}^d}{\gamma_s^d + \gamma_{lv}^d} + \frac{4\gamma_s^p \gamma_{lv}^p}{\gamma_s^p + \gamma_{lv}^p} \qquad (2)$$

Table 2. Surface free energy (γ_{lv}), dispersion (γ_{lv}^d), and polar components (γ_{lv}^p) of test liquids for contact angle measurements.[17]

Test liquids	γ_{lv} (mJ/m^2)	γ_{lv}^d (mJ/m^2)	γ_{lv}^p (mJ/m^2)
Water	72.8	21.8	51.0
Formamide	58.0	39.0	19.0
Diiodomethane	50.8	50.8	0.0

where γ^d was the dispersive and γ^p the polar component of the surface free energy (surface tension), γ_{lv} and γ_s were the surface tension of liquid and the surface free energy of solid, respectively.

Scanning electron microscopy. A SIRION 400 NC scanning electron microscope (SEM) was used to study dispersion of silica particles in iPP/silica composites. This research was performed additionally to the SEM morphology study of iPP/silica composites[15] in order to explain how dispersion and agglomeration of silica particles have affected mechanical properties. Samples were fractured in liquid nitrogen and gold plated before being examined with a microscope at an acceleration voltage up to 10 kV at various magnifications. All SEM micrographs are secondary electron images.

Optical microscopy. A Leica light microscope (Model DMLS) with digital camera was used for observation of thin crossed microtomed sections taken from 1-mm thick plates. A maximal anisotropic diameter of spherulites ($d_{i,max}$) was measured on several polarization micrographs of each sample and an average spherulite diameter (d_{sph}) was calculated according to equation (3)

$$d_{sph} = \frac{\sum N_i d_{i,max}}{\sum N_i} \qquad (3)$$

The results of spherulite diameters have been presented in our previous paper[15] and they are used in this study for determining tensile strength–spherulite size relationships.

Results and discussion

Steady state torque

The mixing torque moment values provide information how silica fillers influence the processability of iPP composites. The torque moment increases by adding polypropylene and silica fillers in batch mixer and decreases after the polypropylene melting and reaches constant value around sixth minute of mixing (measured τ_M values in Figure 1) owing to homogenization and equalized viscosity of composites. Torque moment, τ_M, of all silicas increases with addition of low silica loading as typical result of an increase in filler loading.[2–4] This fact is in accordance with the literature findings that the viscosity usually rises to some critical filler level, which depends upon particle size, shape, interaction with matrix, and amount of agglomeration.[2–4] The τ_M curves display the divergent effect of unmodified polar silica in comparison to modified silicas with further filler loading (Figure 1). Addition of unmodified microsilica S-120 and nanosilica A-200 causes steady increase
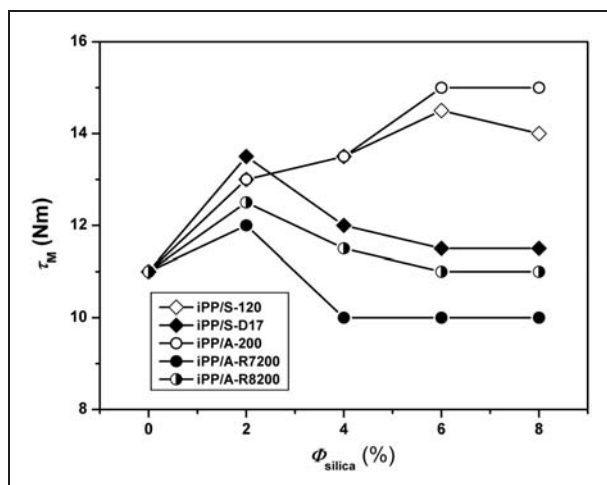
Figure 1. Steady state torque of the iPP/silica composites in dependence on silica content.

Figure 2. Stress–strain curves of the iPP/silica 92/8 composites.

of τ_M values due to increased frictional forces with increased silica content.[2–4,19] If filler and polymer are incompatible, as in the case of hydrophilic silica and a nonpolar iPP polymer, the filler particles are in direct contact with each other.[19–21] Accordingly, higher degree of agglomeration and higher specific surface of hydrophilic nanosilica A-200 than microsilica S-120 lead to higher torque values of the composites with A-200 nanosilica at higher filler content. Silicas with treated surfaces cause after 2 vol% steady decrease of the τ_M to the value for plain iPP or even lower in the case of composites with methacrylsilanized A-R7200 nanosilica (Figure 1). Methacrylsilane with amphiphilic character was applied as coupling agent in literature also for other nanoparticles like $MgCO_3$.[22] Silica particles with modified surface (including A-R7200 with polar carbonyl groups) repel each other and lead to decreased degree of agglomeration. Anyway, coupling agent layer decreases the torque value despite of higher specific surface of finer dispersion. Obviously, filler–filler interactions are still higher than polymer–filler interactions.[23] It is interesting that silica microparticles contribute to the τ_M value more than nanoparticles. Larger effective radii of microparticles and agglomerates lead to higher stress during mixing what results in higher τ_M values for composite with modified S-D17 microsilica than with modified nanosilicas A-R8200 and A-R7200.[10] Torque moment values are in accordance to the interfacial free energy (see further "Interfacial properties of the iPP/silica composites" section) which is significantly higher for composites with hydrophilic A-200 and S-120 fillers than with modified S-D17, A-R8200, and A-R7200 silicas. Torque value of composite with S-D17 exhibiting minimal interfacial free energy value ($9.8\,mJ/m^2$) seems to be
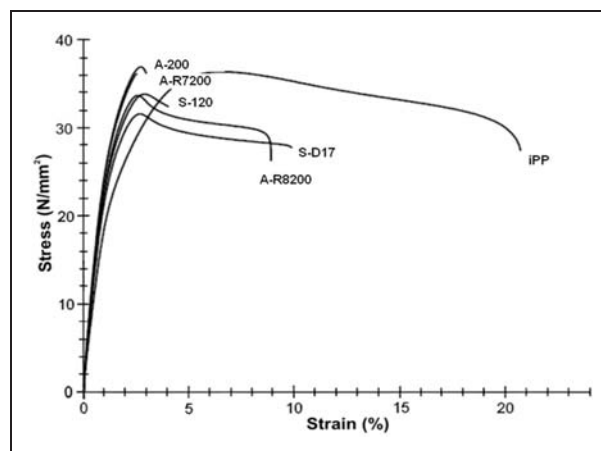
compensated by effect of larger effective radii of S-D17 microparticles.

Tensile test

Mechanical properties of reinforced polymer–matrix composites are primarily influenced by component properties and interfacial interaction between the polymer matrix and the filler surface as well as by the ultimate morphology of composites.[2,3]

Stress–strain curve. The introduction of silica fillers into neat iPP changes the fracture character from relatively ductile (neat iPP) to a brittle fracture (iPP/silica 92/8 composites) as stress–strain curves shown in Figure 2. The decrease in ductility is a result of the reinforcing effect of silica filler. However, the iPP composites with treated, hydrophobic surfaces of silica fillers (S-D17 and A-R8200) exhibit the higher ductility in comparison to other silica fillers. This fact corresponds to the findings of remarkably high spherulite size in the iPP composites with S-D17 and A-R8200 as a result of better compatibility of these silica fillers with iPP matrix compared to other fillers.[15] Maximal stress, σ_{max} of the composites (Figure 2) corresponds mainly to yield stress value, σ_y, due to the shape of the stress–strain curves; therefore, only tensile strength values at yield and at break were presented.

Young's modulus. Young's modulus steadily rises with increased filler content (Figure 3) due to reinforcing or stiffening effect of filler also observed in papers with similar binary iPP/nanosilica composites.[6–9] Interesting observation is the E values decrease of the composites with 8 vol% of added silicas in the following order: A-200 > A-R7200 > A-R8200 > S-120 > S-D17. Higher moduli of the composites with
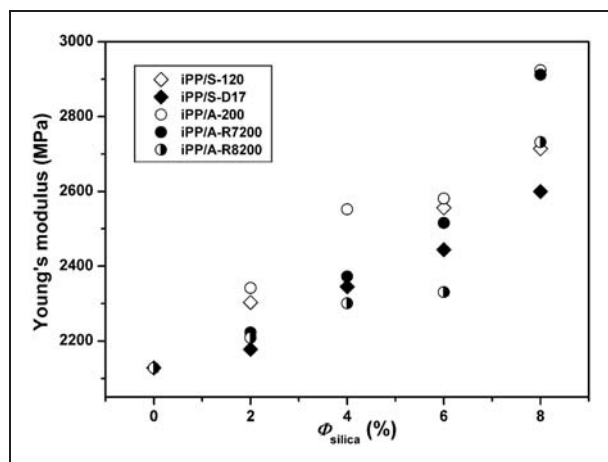
Figure 3. Young's modulus of the iPP/silica composites in dependence on silica content.

nanosilica than microsilica may indicate pronouncing influence of interfacial surface or agglomeration extent: higher values for iPP/nanosilica than at iPP/microsilica interfaces in composites with increased silica content. Since the agglomeration in composites with nanosilica is observed in a smaller extent than in composites with microfillers (finer dispersion of smaller particles) and the aggregates are smaller in size, the nanocomposites have higher stiffness than microcomposites.[23]

Moreover, composites with polar silicas (A-200, A-R7200, and S-120) exhibit higher E values than corresponding composites with nonpolar silicas (A-R8200 and S-D17). It seems that polar silica causes additional stiffening and reinforcing effect of polypropylene matrix due to its high nucleating ability what consequently leads to the morphology with smaller spherulites.[15]

Yield stress and strain. The yield stress gives additional information on filler–polymer matrix interactions, besides the information about strength of material before it suffers macroscopic plastic deformation.[2,3] The composites with polar A-200 and A-R7200 nanosilicas exhibit significantly higher σ_y values than the composites with S-120, S-D17, and A-R8200 silica fillers (Figure 4(a)). The σ_y behavior may be related with the spherulite size and the spherulite boundaries effect[24,25] (small spherulites in composites with A-200 and A-R7200 against large spherulites in composites with S-D17 and A-R8200).[15] However, low σ_y values for both composites with unmodified S-120 and modified S-D17 silicas may indicate the effect of either specific interfacial surface (especially particle size) or dispersion quality (common for composites with both microsilicas and A-R8200 nanosilica) on yield stress. The values of interactive parameter B, evaluated from
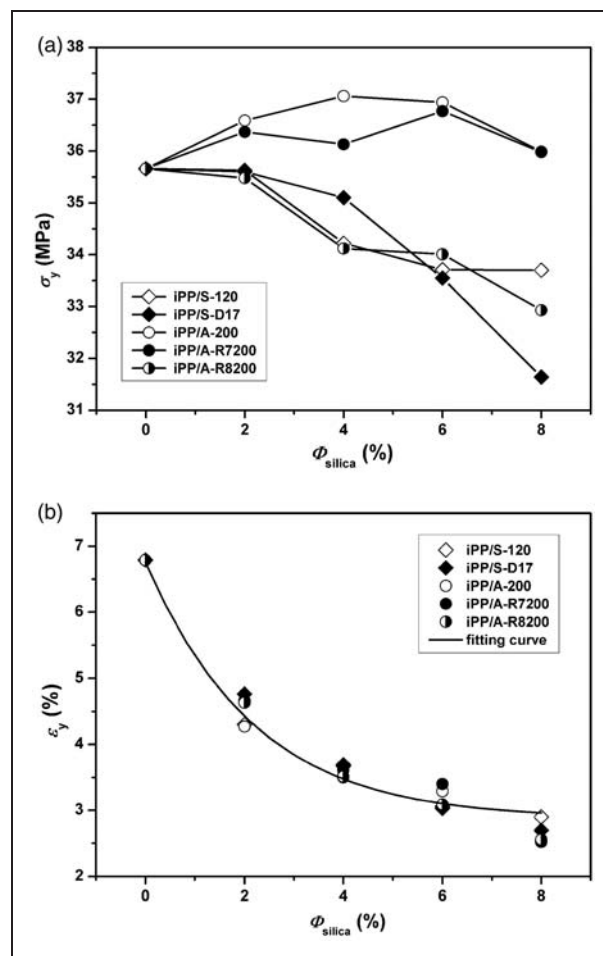

Figure 4. Yield stress (a) and yield strain (b) of the iPP/silica composites in dependence on silica content.

Table 3. Interaction parameter B of the iPP/silica composites.

iPP/silica composite	Interaction parameter B
iPP/S-120	2.55
iPP/S-D17	2.19
iPP/A-200	3.76
iPP/A-R7200	3.64
iPP/A-R8200	2.42

σ_y values, are in good accordance with the calculated adhesion parameters (Table 3).

The elongation at yield, ε_y, of neat semicrystalline iPP depends on the strengthening of tie molecules, intercrystalline and interspherulitic links before stretching of composite test specimen. The incorporation of silica filler into neat iPP decreases the elongation at yield due to reinforcing effect of the silica particles and resembles to similar ε_y- values behavior (Figure 4(b)). Rapid decrease of the ε_y values at

2 vol% of added silicas correlates with the findings that the spherulites with reduced size may decrease elongation at yield according to the Hall–Petch law.[26] Relatively low yield strain of all composites with 8 vol% silica filler corresponds to the additional deterioration of other mechanical properties discussed later. It could also be related with increased agglomeration of silica particles and lower degree of crystallinity[15] in composites with 8 vol% of silica filler.

The results of the interaction parameter B are presented in Table 3. Because they are calculated on the basis of σ_y values, their behavior and explanation are similar as in the case of yield stress values: higher B values for composites with A-200 and A-R7200 nanofillers ($B = 3.76$ and 3.64, respectively) in comparison to composites S-120 microsilica ($B = 2.55$) and with nonpolar S-D17 and A-R8200 ($B = 2.19$ and 2.42, respectively).

It seems that σ_y and B values are influenced by surface characteristics, particle size, and dispersion quality in a complex way. The parameter B showed very good concordance with calculated adhesion parameters in present iPP/silica composites.

Tensile strength and elongation at break. Incorporation of different fillers into polymers affects tensile strength at break, σ_b, differently; it usually increases or decreases σ_b values, whereas some fillers behave without visible effect.[2,3] The addition of 2 vol% of all silica grades remarkably increases tensile strength at break (Figure 5(a)). Maximal σ_b values obtained mainly in the range 2–6 vol% of added silicas are in line with literature values obtained for the iPP composites with grafted nanosilica particles.[7,8] Afterwards these concentration range σ_b values stagnate due to increased agglomeration and decreased crystallinity.[15] The σ_b values (Figure 5(a)) exhibited more pronounced differences with the increased silica content than σ_y values (Figure 4(a)). The σ_b values of the composites with 8 vol% of added silicas decrease in the following order: A-R7200 > A-200 > S-120 > S-D17 > A-R8200. The difference σ_y–σ_b, as a measure for ductility,[9] decreases in inverse order: iPP > A-R8200 > S-D17 > S-120, A-200 > A-R7200. Similar behavior is observed in spherulite size change discussed through tensile strength–spherulite size relationship.

Addition of 2 vol% of silica to plain iPP decreases ε_b values rapidly (Figure 5(b)). The elongation at break, ε_b, usually behaves inversely to the tensile strength at break, σ_b. However, there are small, but observable differences between ε_b behaviors of composites with nonpolar and with polar silicas. Composites with polar S-120, A-200, and A-R7200 silica fillers and common characteristic of small spherulites[15] exhibit monotonic, almost linear decrease of ε_b values.
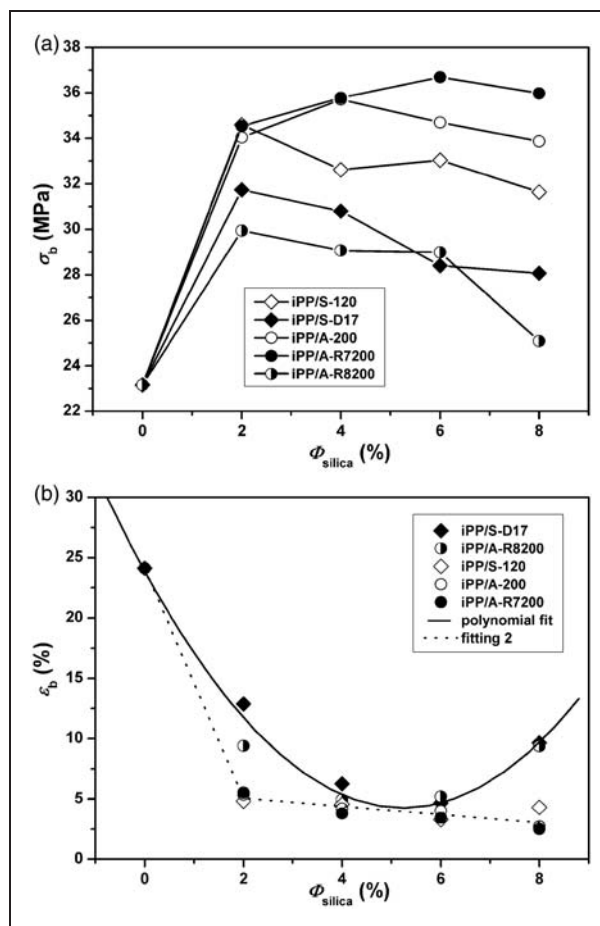

Figure 5. Tensile strength (a) and elongation (b) at break of the iPP/silica composites in dependence on silica content.

On the other hand, ε_b values of composites with nonpolar S-D17 and A-R8200 silicas and common characteristic of large spherulites[15] obey polynomial fitting satisfactorily. Unexpected increase of the ε_b values at 8 vol% of nonpolar silica could be attributed to still regular spherulites[27] due to decreased nucleation ability of enlarged aggregates in the iPP matrix according to Zou et al.[28] On the other side, modified S-D17 microparticles and A-R8200 aggregates/agglomerates with finer dispersion than other silica fillers could be more suitably accommodated in interspherulitic regions[15] and with improved interactions with compatible iPP matrix. All composites are ductile materials because ε_b values in Figure 5(b) are mainly higher than limit fracture strain of 2–3%.[27] The simultaneous decrease of σ_b and ε_b values of composites with 8 vol% of polar silicas could be related to some additional factors discussed in tensile strength–spherulite size relationships.

Tensile strength–spherulite size relationships. In order to establish how restructured iPP matrix (spherulite size)

affected tensile strength of iPP/silica composites, the tensile strength–spherulite size relationship was studied. Large spherulites in composites with nonpolar S-D17 and A-R8200 silica fillers arose because of weak nucleation effect of nonpolar silica particles that are compatible or miscible with nonpolar iPP chains. Ray et al.[29] proved that lower primary and proposed secondary nucleation density of the crystallites in poly((butylene succinate)-*co*-adipate) with more miscible filler cloisite*30B than cloisite*20 A led to significantly enlarged spherulites. Accordingly, composites with larger iPP spherulites exhibit higher ductility and correspondingly lower σ_y and σ_b values than the composites with smaller spherulites (with polar silicas A-R7200, A-200, and S-120). Dependence of the tensile yield and break strength values on the spherulite size was shown in Figure 6(a) and (b), respectively (curves were fitted for every silica content separately). The correlation factors for σ_b–d_{sph} relations (Figure 6(b)) are higher than those–for σ_y–d_{sph} relations (Figure 6(a)). Although the correlation factor fluctuates, both the graphs (σ_y–d_{sph} and σ_b–d_{sph}) exhibit similar behaviors; σ_y and σ_b values decrease with increased spherulite size. This fact is in accordance to the literature findings that the yield stress increases with decreasing spherulite size and with strengthening of the spherulite boundaries.[24,25] Moreover, σ_y–d_{sph} and σ_b–d_{sph} line slopes decline clockwisely with increased silica content. Remarkable distinction in observed slopes between composites with 8 vol% and those with 2–6 vol% indicates phenomenological difference between these two groups of composites. Composites with 2–6 vol% of silicas exhibit slower decrease of σ_y–d_{sph} and σ_b–d_{sph} values than composites with 8 vol% of silica. Fast dip of both σ_y–d_{sph} and σ_b–d_{sph} lines at 8 vol% of silicas indicates additional deteriorating factors that weaken the matrix and the whole composite specimen. This could be ascribed to the difference in strength of regular versus small coarsened spherulites or to significantly weakened interspherulitic boundaries below a certain spherulite size.[30]

Significant differences in σ_y–d_{sph} and σ_b–d_{sph} behavior of composites with 8 vol% of added silica in comparison to the composites with 2–6 vol% of silicas could be related with crystallinity changes observed in previous paper.[15] Determined degrees of crystallinity for composites with 2–6 vol% of silicas[15] are in accordance with theoretical values linearity within the method resolution.

The highest decrease in crystallinity observed in composites with 8 vol% of silicas[15] could be related to fast dip of tensile strengths with changed crystallinity in addition to spherulite size (Figure 6(a) and (b)). However, the difference in relevancy of applied methods should be mentioned: spherulites were observed in
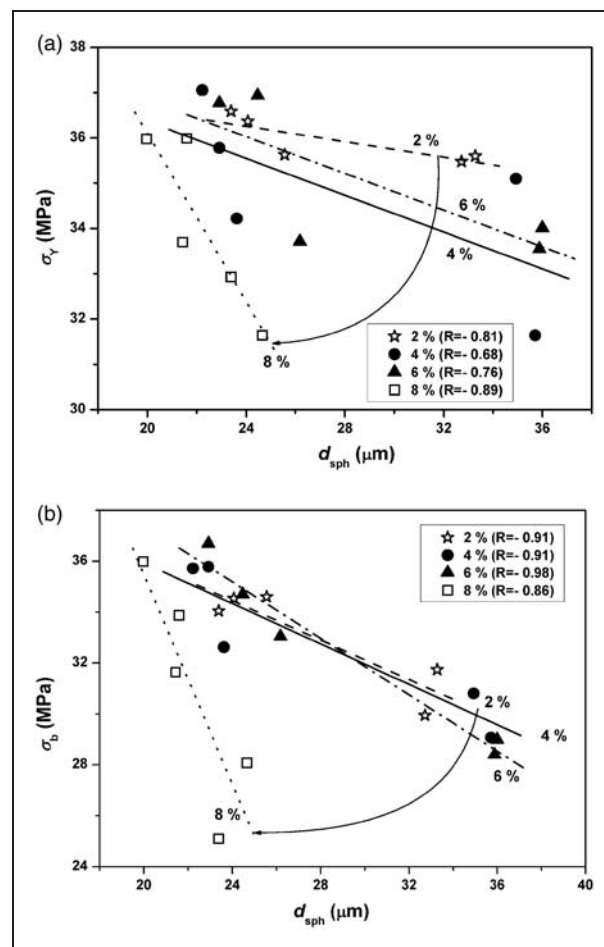

Figure 6. Tensile strength at yield (a) and break (b) of the iPP/silica composites in dependence on spherulite size. Every point corresponds to point in Figures 4(a) and 5(a). R is correlation factor relating to composites with the same silica content: 2, 4, 6, and 8%.

thin slices (practically 2D layers) by polarization microscopy while the crystallinity was determined from bulk samples (1-mm-thick films) by wide angle X-ray diffraction (WAXD). Because the spherulite size and crystallinity are interdependent to some extent (small spherulites mainly imply low crystallinity) the resolution of particular influence of spherulite size or crystallinity is hardly achievable.

Moreover, increased degree of agglomeration and steric hindrances of silica particles may also have influence on such behavior.[6,31] Comparison of nanosilica dispersions in previous paper[15] indicates somewhat better distribution and finer dispersion of modified (A-R8200) than hydrophilic (A-200) silicas in the iPP matrix. Additional research was carried out to analyze how the quality of dispersion has been changed with increased filler loading. SEM micrographs in Figure 7(a) to (d) reveal the growth of aggregates and agglomerates of silica nanoparticles with the increased
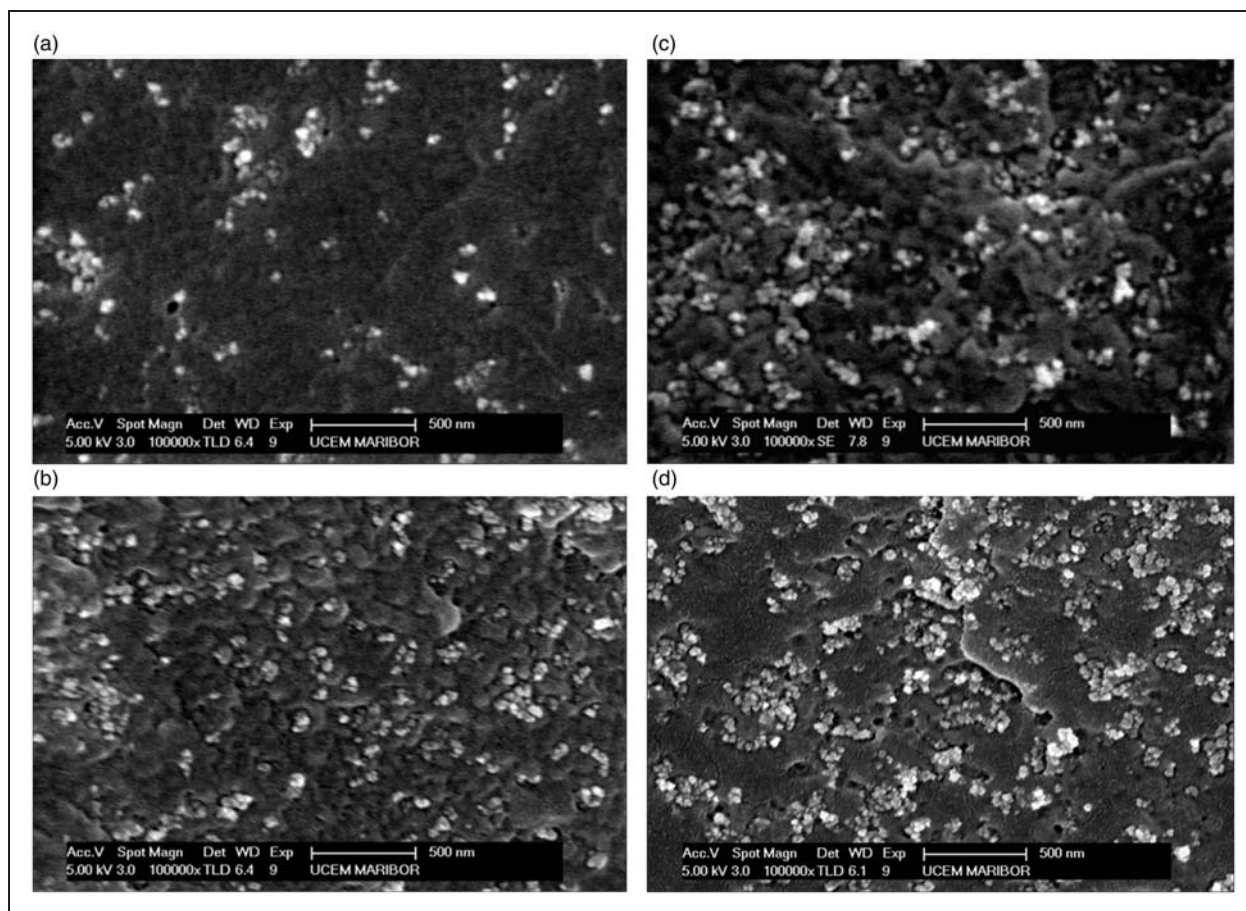
Figure 7. SEM micrographs of the iPP composites with 2 vol% (a), 4 vol% (b), 6 vol% (c), and 8 vol% (d) of nanosilica A-R8200.

silica content even in composites with nonpolar A-R8200 silica nanoparticles (the lowest σ_b values in Figure 5(a)). The difference in agglomeration with increased silica content (Figure 7(a) to (d)) is more significant than the difference between different nanosilica grades.[15] These results are in accordance with findings in literature that agglomeration of silica nanoparticles deteriorates the mechanical properties.[6,9] Nonpolar A-R8200 and S-D17 fillers have the weakest nucleation ability due to good compatibility with the iPP matrix causing more ductile iPP matrix with the largest spherulites. Large A-R8200 (Figure 7(d)) (and other nanosilicas) agglomerates decrease the crystallinity[15] what might decrease tensile strength at 8 vol% additionally.

Impact properties

Since the numerous factors (particle size and rigidity, filler aspect ratio, structural changes in polymer matrix, etc.) affect the impact strength of polymer composites, it is difficult to resolve and to determine the influence of particular factor and to predict how addition of filler changes the impact strength.[2] The impact strength
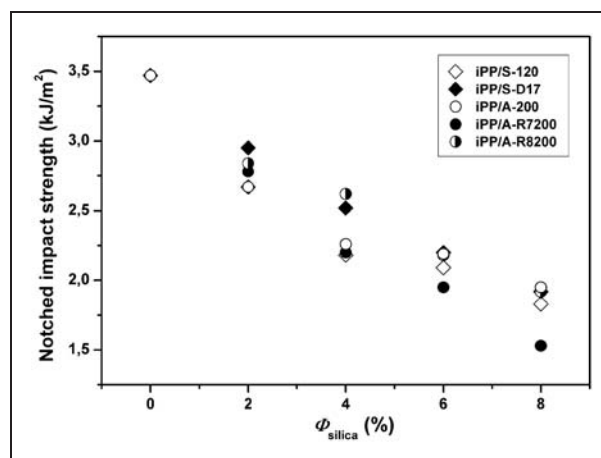

Figure 8. Notched impact strength of the iPP/silica composites in dependence on silica content.

values, a_K, decrease monotonously with addition of the silica fillers (Figure 8). Steady decrease could indicate that the silica fillers act primarily as harder particles that affected Young's modulus (Figure 3), failure

Table 4. The surface free energy (γ) of the iPP and different silica fillers and their dispersive (γ^d) and polar component values (γ^p) evaluated by using the Wu's model.[18]

Sample	The surface free energies (mJ/m^2)		
	γ^d	γ^p	γ
iPP	31.5	1.3	32.8
Sipernat 120	37.6	37.0	74.6
Sipernat D17	7.3	0.0	7.3
Aerosil 200	39.6	37.1	76.7
Aerosil R7200	43.4	17.8	61.2
Aerosil R8200	3.2	0.0	3.2

mode, and toughness. Somewhat stronger decrease of the a_K values at 2 vol% of silicas is in accordance with the decrease of the ε_b and ε_b values. It is interesting that the composites with the highest τ_M values (A-200 and S-120 in Figure 1) and the highest ε_b values (S-D17 and A-R8200 in Figure 5(b)) at 8 vol% of silicas exhibit higher a_K values than corresponding composite with A-R7200.

Interfacial properties of the iPP/silica composites

Study of the adhesion phenomena and the interaction in composites is suitable for composite engineering because morphology and mechanical properties of polymer composites strongly depend on interfacial properties between components.[23,32] The calculations of the adhesion parameters from surface free energies of the components and the interaction parameter values from yield stress values enable prediction of the interfacial properties and their influence on the mechanical properties.

Contact angle measurement is a standard method for evaluating the surface free energies, γ of solids[32] with, respectively, dispersive, γ^d and polar component, γ^p values calculated from standard test liquids by using the Wu's harmonic mean equation.[18]

The results of surface free energy for iPP and silica fillers exhibit low polar component value of the surface free energy of the iPP and only dispersive contribution to the surface free energy for microsilica S-D17 and nanosilica A-R8200 (Table 4).

The distinctive nonpolar nature of these fillers is a result of chemical termination of –OH groups on silica particles surface with chemically bonded carbon in case of S-D17 microsilica and with hexamethyl-disilazane in case of A-R8200 nanosilica. Better similarity in the surface free energy of nonpolar iPP matrix with nonpolar S-D17 and A-R8200 fillers than with polar silicas (S-120, A-200, A-R7200) implies more miscible or compatible interfaces in iPP/nonpolar silica than iPP/polar silicas. These results are in line with lower interaction

parameter B of the composites with nonpolar S-D17 and A-R8200 fillers (Table 3). More compatible iPP–silica interface and the morphology with larger spherulites[15] in composites with S-D17 and A-R8200 lead to higher ductility (Figure 2) and lower tensile strengths σ_y and σ_b values (Figures 4 and 6). Despite the surface of the nanosilica A-R7200 was modified with methacrylsilane, it exhibits higher dispersive and more polar component than A-R8200 probably because of polar carbonyl C=O groups in methacrysilane layer. Anyway, nanosilica A-R7200 has the strongest nucleation ability among all used silica fillers that causes the smallest spherulites or even the morphology with dark branched grains without Maltese crosses.[15] Specific irregular morphology together with relatively fine dispersion of A-R7200 seems to cause superb tensile strength behavior of composites with A-R7200 nanofiller. Relatively high values of the surface free energy and its polar component of microsilica S-120 and nanosilica A-200 fillers originate from, among other, polar nonterminated –OH groups on silica particles. Both fillers, as strong nucleators, cause small spherulites. However, somewhat higher γ values for A-200 nanosilica than S-120 microsilica filler could be ascribed to higher specific surface of A-200 nanoparticles than S-120 microparticles. Similarly, low σ_y values for composites with S-120 and S-D17 microsilicas (with similar surfaces) confirm the effect of specific surface on mechanical properties (see Figure 4(a)).

Adhesion parameters such as the work of adhesion, W_{mf}, the interfacial free energy, γ_{mf}, and the spreading coefficient (coefficient of wetting), S_{mf}, were used to predict the adhesion strength of possible pairs in polypropylene/silica composites and their influence on morphology and mechanical properties. The adhesion parameters were calculated according to following equations (4) to (6)[32]

$$W_{mf} = \gamma_f + \gamma_m + \gamma_{mf} \tag{4}$$

$$\gamma_{mf} = \gamma_f + \gamma_m - 2\sqrt{\gamma_f^d \gamma_m^d} - 2\sqrt{\gamma_f^p \gamma_m^p} \tag{5}$$

$$S_{mf} = \gamma_f - \gamma_m - \gamma_{mf} \tag{6}$$

where subscripts m and f mean matrix and filler, and superscripts d and p their dispersive and polar components, respectively.

The results of the studies on the effective adhesion for a given system indicate some conditions as optimal: the thermodynamic work of adhesion as maximal, the spreading coefficient as a positive value, and the interfacial free energy as a minimal one.[32] Higher values of the work of adhesion and the spreading coefficient in

Table 5. Adhesion parameters γ_{mf}, W_{mf}, S_{mf} of the iPP/silica composites.

Composite	Adhesion parameters (mJ/m^2)		
	Interfacial free energy, γ_{mf}	Work of adhesion, W_{mf}	Spreading coefficient, S_{mf}
iPP/S-120	24.7	82.7	17.1
iPP/S-D17	9.8	30.3	−35.3
iPP/A-200	24.9	84.5	18.9
iPP/A-R7200	10.4	83.6	18.0
iPP/A-R8200	15.9	20.1	−45.5

iPP composites with microsilica S-120, and nanosilica A-200 and A-R7200 indicate the presence of significant interactions at the iPP–silica interfaces in these composites (Table 5).

Negative spreading coefficient values of the composites with S-D17 and A-R8200 silica fillers that are treated with chemically bonded carbon (S-D17) and hexamethyl-disilazane (A-R8200) indicate low wettability and low interactivity at iPP matrix–filler interface as a consequence of the filler surface treatment. At the same time, low surface free energy values at the interfaces point to more miscible/compatible iPP matrix with these two fillers (Table 5). Composites with the hydrophilic A-200 nanosilica exhibit higher thermodynamic work of adhesion W_{mf} and spreading coefficient S_{mf} than S-120 microsilica what is in accordance with steady increase of their τ_M values (Figure 1).

Generally, the fillers with untreated surfaces (S-120 and A-200) and with distinct hydrophilic character have shown more effective adhesion and assumed stronger nucleation ability. Accordingly, the surface properties of silica fillers have influenced not only the crystallization and spherulite size of polypropylene matrix, but also have affected ultimate tensile strength properties on rather unexpected way with distinction for silica content up to 6 vol% and with 8 vol%.

Conclusions

Interfacial properties of the iPP/silica composites were primarily determined by the surface character of silica particles, namely by the adhesion parameters of possible polypropylene/silica pairs in composites. Generally, silicas with the unmodified hydrophilic surfaces (S-120 and A-200) exhibited effective adhesion and strong nucleation ability that led to smaller spherulites and to better tensile strength behavior. Nanosilica A-R7200 modified with methacrylsilane has shown similar tensile strength behavior. Pretreatment of filler surface with chemically bonded carbon (S-D17) and

hexamethyl-disilazane (A-R8200) results in relatively high miscibility/compatibility with iPP chains, low torque moment, large spherulites, higher ductility, and lower tensile strength in comparison to the iPP composites with other fillers. Mechanical behaviors of composites might be additionally influenced by the reinforcing character of silica fillers, the dispersion of filler in polypropylene matrix, silica content, and reduced mobility of macromolecules due to interaction between filler particles and the iPP chains. All influencing factors differently affect mechanical behavior of composites within silica content range from 2 to 6 vol% and with 8 vol% of added silica.

Conflict of interest

None declared.

References

1. Wagner MP. Natural and synthetic silicas in plastics. In: Seymour RB (ed.) *Additives for plastics*. Vol. 1, New York: Academic Press, 1978, pp.9–28.
2. Rothon RN. *Particulate-filled polymer composites*, 2nd ed. Shawbury: Rapra Technology, 2006.
3. Wypych G. *Handbook of fillers*, 2nd ed. Toronto: ChemTec Publishing, 2000.
4. Karian HG. Preface. In: Karian HG (ed.) *Handbook of polypropylene and polypropylene composites*. New York: Marcel Dekker, 1999.
5. Karger-Kocsis J and Fakirov S. Preface. In: Karger-Kocsis J and Fakirov S (eds) *Nano- and micromechanics of polymer blends and composites*. Munich: Carl Hanser Verlag, 2009.
6. Bikiaris DN, Papageorgiou GZ, Pavlidou E, et al. Preparation by melt mixing and characterization of isotactic polypropylene/SiO$_2$ nanocomposites containing untreated and surface-treated nanoparticles. *J Appl Polym Sci* 2006; 100: 2684–2696.
7. Rong MZ, Zhang MQ, Zheng YX, et al. Structure–property relationships of irradiation grafted nano-inorganic particle filled polypropylene composites. *Polymer* 2001; 42: 167–183.
8. Wu CL, Zhang MQ, Rong MZ, et al. Tensile performance improvement of low nanoparticles filled-polypropylene composites. *Compos Sci Technol* 2002; 62: 1327–1340.

9. Vassiliou A, Bikiaris DN and Pavlidou E. Optimizing melt-processing conditions for the preparation of iPP/fumed silica nanocomposites: Morphology, mechanical and gas permeability properties. *Macromol React Eng* 2007; 1: 488–501.

10. Šišakova J. Polymer materials and its properties. In: Er MJ (ed.) *New trends in technologies: Devices, computer, communication and industrial systems*. Rijeka: InTech, 2010, pp.15–42.

11. Papanicolau GC and Bakos D. The influence of the adhesion bond between matrix and filler on the tensile strength of particulate-filled polymers. *J Reinf Plast Compos* 1992; 2: 104–126.

12. Galeski A and Regnier G. Nano- and micromechanics of crystalline polymers. In: Karger-Kocsis J and Fakirov S (eds) *Nano- and micromechanics of polymer blends and composites*. Munich: Carl Hanser Verlag, 2009.

13. Huang L, Zhan R and Lu Y. Mechanical properties and crystallization behavior of polypropylene/nano-SiO$_2$ composites. *J Reinf Plast Compos* 2006; 25: 1001–1012.

14. Zaman HU, Hun PD, Khan RA, et al. Morphology, mechanical, and crystallization behaviors of micro- and nano-ZnO filled polypropylene composites. *J Reinf Plast Compos* 2012; 31: 323–329.

15. Pustak A, Pucić I, Denac M, et al. Morphology of polypropylene/silica nano- and microcomposites. *J Appl Polym Sci* 2013; 128: 3099–3106.

16. Turcsányi B, Pukánszky B and Tudos F. Composition dependence of tensile yield stress in filled polymers. *J Mater Sci Lett* 1988; 7: 160–162.

17. van Oss CJ, Giese RF, Li Z, et al. Determination of contact angles and pore sizes of porous media by column and thin layer wicking. In: Mittal KL (ed.) *Contact angle, wettability and adhesion*. Utrecht: VSP, 1993, pp.269–284.

18. Wu S. Polar and nonpolar interaction and nonpolar interaction in adhesion. *J Adhes* 1973; 5: 39–55.

19. Dierkes W. *Economic mixing of silica-rubber compounds. Interaction between the chemistry of the silica-silane reaction and the physics of mixing*. PhD Thesis, University of Twente, 2005.

20. Wang K, Wu JS and Zeng H. Radial growth rate of spherulites in polypropylene/barium sulfate composites. *Eur Polym J* 2003; 39: 1647–1652.

21. Derksen JJ and Eskin D. Flow-induced forces in agglomerates. *Fluid Dyn Mater Process* 2011; 7: 341–355.

22. Siengchen S and Karger-Kocsis J. Polystyrene nanocomposites produced by melt-compounding with polymer-coated magnesium carbonate nanoparticles. *J Reinf Plast Compos* 2012; 31: 145–152.

23. Moczo J and Pukanszky B. Polymer micro and nanocomposites: Structure, interaction, properties. *J Ind Eng Chem* 2008; 14: 535–563.

24. Way JL, Atkinson JR and Nutting J. The effect of spherulite size on the fracture morphology of polypropylene. *J Mater Sci* 1974; 9: 293–299.

25. Friedrich K. Strength and fracture of crystalline isotactic polypropylene and the effect of molecular and morphological parameters. *Prog Colloid Polym Sci* 1979; 66: 299–309.

26. Martins JA, Cramez MC, Oliveira MJ, et al. Prediction of spherulite size in rotationally molded polypropylene. *J Macromol Sci Part B Phys* 2003; 42: 367–385.

27. Bazhenov S. Mechanical behavior of filled thermoplastic polymers. In: Cuppoletti J (ed.) *Metal, ceramic and polymeric composites for various uses*. Rijeka: InTech, 2011, pp.171–195.

28. Zou H, Wu S and Shen J. Polymer/silica nanocomposites: Preparation, characterization, properties, and applications. *Chem Rev* 2008; 108: 3893–3957.

29. Ray SS, Bandyopadhyay J and Bousmina M. Influence of degree of intercalation on the crystal growth kinetics of poly[(butylene succinate)-co-adipate] nanocomposites. *Eur Polym J* 2008; 44: 3133–3145.

30. Ouederni M and Phillips PJ. Influence of morphology on the fracture, toughness of isotactic polypropylene. *J Polym Sci Polym Phys Ed* 1995; 33: 1313–1322.

31. Manias E, Polizos G, Nakajima H, et al. Fundamentals of polymer nanocomposite technology. In: Morgan AB and Wilkie CA (eds) *Flame retardant polymer nanocomposites*. Hoboken: Wiley-Interscience, 2007, pp.31–66.

32. Mittal KL. The role of the interface in adhesion phenomena. *Polym Eng Sci* 1977; 17: 467–673.

Appendix 1

Notation

a_K	notched impact strength
B	interaction parameter
d	average particle size
d_{sph}	average spherulite diameter
E	Young's modulus
N_i	number of spherulite
S	spreading (wetting) coefficient
W	work of adhesion
γ	surface (interfacial) free energy
ε_b	elongation at break
ε_y	yield strain
λ	electrolytic conductivity
ρ	density
σ_b	tensile strength at break
σ_y	yield stress
τ_M	steady state torque moment
ϕ	volume fraction